

Velocity and BottomStress Measurements in the Bottom Boundary Layer,
Outer Norton Sound, Alaska

David A. **Cacchione**

David E. Drake

Patricia **Wiberg**

U.S. Geological Survey

Menlo Park, California 94025

Abstract

We have used long-term measurements of near-bottom velocities **at** four heights **above the sea floor in** Norton Sound, Alaska, to compute hourly values of shear velocity u_* , roughness Z_0 , and bottom-drag coefficient C_D . Maximum sediment resuspension and transport, predicted for periods when the computed value of u_* exceeds a critical level, occur during peak tidal currents associated with spring tides. The **fortnightly** variation in u^* is correlated with a distinct **nepheloid** layer that intensifies and thickens during spring tides and diminishes and thins during neap tides. The passage of a storm near the end of the experiment caused significantly higher u^* values than those found during fair weather. We attribute these increases **in u_* to** stronger **bottom currents** and larger surface waves.

INTRODUCTION

The most important dynamic parameter controlling the transport of sediment in the **bottom** boundary layer over continental shelves is the **bottom** shear stress τ_b . Historically, most estimates of τ_b in both natural and laboratory settings have been made by measuring the flow velocity at one or more heights above the bottom and applying an appropriate boundary-layer equation that relates the bottom shear stress to the velocity field. For example, in steady unidirectional turbulent flow over a flat bed whose only bottom irregularities are uniform sand grains, τ_b can be calculated from the relations (Schlichting, 1968):

$$\tau_b = \rho u_{*b}^2, \quad (1a)$$

$$\text{and } \frac{u}{u_{*b}} = \frac{1}{k} \ln(z/z_0), \quad (1b)$$

where u is the current speed at a height z above the **bottom**, ρ is the fluid density, k is von **Karman's** constant (0.4), u_{*b} is the bottom shear velocity, and Z_0 is a roughness parameter. Equation (1b) applies within the turbulent **lower** part of the velocity profile, commonly referred to as the logarithmic zone; over continental **shelves**, this zone is within about 10 m of the sea **floor** (Wimbush, 1976). Sternberg (1968) found that approximately 85 percent of the vertical velocity distributions measured in six different tidal channels **fit the** logarithmic velocity profile given by equation (1b). Other velocity-profile measurements in dominantly shallow tidal flows also demonstrate the applicability of equation (1b) in estimating u_{*b}

(Bowden and others, 1959; **McCave, 1973**; Smith and McLean, 1977).

Two major difficulties that arise in applying equation (1b) to natural boundary-layer flows involve situations (1) where bottom irregularities or bed features exist whose vertical length scales exceed that of the sedimentary grains at the bed surface, and (2) when active sediment transport of bed load and near-bottom suspended load occurs. Smith and McLean (1977), who considered these problems, presented methods for dealing with the changes in shear velocity u_* that result. In particular, when more than one vertical scale of bed roughness is present, Smith and McLean argued that the velocity profile is separated into vertical zones that reflect the scales of these roughness elements. They suggested that equation (1b) applies within each vertical zone and that Z_0 for that zone is related to a particular physical roughness scale. For example, if the bottom consists of well-sorted sand grains and regularly spaced asymmetric sediment ripples, the slope of the velocity profile above these features changes at a height determined by the transition from a layer dominated by skin friction over the individual sand grains to an upper layer in which the form drag imposed by sediment ripples on the flow is dominant. This change in the velocity profile signifies a corresponding change in u_* and Z_0 , which in the lowest layer (where $u_* = u_{*b}$) are the appropriate parameters associated with skin friction acting on the surficial sedimentary grains.

When u_{*b} exceeds the value necessary to initiate bed-load transport, Z_0 is effectively proportional to the excess shear stress (Smith and McLean, 1977) and exceeds the values of Z_0 commonly given for turbulent boundary layers (Schlichting, 1968).

An additional problem **in** estimating u_* at the sea floor arises when surface waves generate bottom velocities (and stresses) that are of magnitudes comparable to those typical of the mean flow. Smith (1977) and Grant and Madsen (1979) showed that the wave and current stresses are nonlinearly coupled and that the net effect is to increase the mean stress above the value **it** would have if **waves were** absent. Both Smith (1977) and Grant and Madsen (1979) also showed that z_0 values derived from velocity-profile measurements when waves and quasi-steady currents are both significant are increased by wave-current interaction. Grant and Madsen suggested that some of the anomalously high values of z_0 reported by other researchers can be explained by this effect.

The estimates of u^* reported here were derived by the logarithmic-profile method, using measurements of near-bottom current velocities on an open continental shelf. The **data were** collected in outer Norton Sound, Alaska, during an 80-day period from July 8 to September 26, 1977, using an instrumented, in-situ bottom tripod (**GEOPROBE**; Fig. 1).

Cacchione and Drake (1980) and Drake and others (1980) have documented the importance of late-summer, early-fall storms in causing high rates of sediment transport throughout outer Norton Sound. They found **that storm-** driven bottom stresses are often large enough to resuspend **surficial** deposits at the GEOPROBE site and thereby enhance removal of these deposits by the regional northward flow. In addition, Drake and others (1980) also argue that during the more persistent fair-weather regime, tidal bottom stresses are significant in the near-bottom transport of sediment derived from the Yukon

River (Fig. 1), which occurs at relatively lower rates than during storms but over prolonged durations.

In this report we discuss the variation of u_* during fair-weather periods and emphasize the **diurnal** and fortnightly tidal influence. We also include brief discussion of additional contributions to u_* during periods of high surface **waves**. **Cacchione** and Drake (1980) have already used these data to show the influence **of stresses** due to surface waves on mean **or** quasi-steady stress, **as** predicted by the theoretical formulations of Smith (1977) and Grant and Madsen (1979).

METHODS

The GEOPROBE system is an instrumented tripod designed to make onsite near-bottom measurements of currents, **pressure**, temperature, and light transmission and scattering, and to photograph the sea floor over durations of about 3 months (**Cacchione** and Drake, 1979). During 1977 the **GEOPROBE** was deployed in Norton Sound in 18-m mean water depth about 60 km south of **Nome**, Alaska (Fig. 1). Data were obtained at a basic interval of 1 h over a 3-mo period and recorded on a digital cassette tape. Two orthogonal components of horizontal current were measured with spherical **electromagnetic** (e-m) current sensors **at** four heights-- 20, 50, 70, and 100 cm--above the sea floor (**Cacchione** and Drake, 1979). At the hourly basic intervals, each component **of** current **was** sampled in a burst mode, once each second for a one-minute duration; bottom pressure was sampled at the same rate. Current speed and direction were measured with a **Savonius** rotor and vane, respectively, at hourly intervals. These latter measurements provided a consistency check on the e-m current-meter data.

The **e-m current-meter** data were **treated as** follows. First, individual pairs of velocity component measurements, u_i and v_i , at each vertical level were rotated to provide north-south (v) and east-west (u) components. The rotation angle was determined from photographs of an underwater compass mounted on the **GEOPROBE** and was corrected for magnetic declination; the accuracy of this procedure is about $\pm 5^\circ$.

Burst means (\bar{u}, \bar{v}) for each component were then calculated over the one-minute sample durations:

$$\bar{u} = \sum_{i=1}^{60} u_i ; \bar{v} = \sum_{i=1}^{60} v_i \quad (2)$$

Burst mean current speed s and burst mean current direction θ were also computed for each one-minute burst:

$$s = (\bar{u}^2 + \bar{v}^2)^{1/2} ; \theta = \tan^{-1} \frac{\bar{v}}{\bar{u}} \quad (3)$$

A total of 1,920 values of s and θ were thus obtained over the 3-month experiment. The s values **compared** favorably with the hourly current speeds measured with the Savonius rotor, except during periods of relatively high surface waves (wave heights > 1 m), when rotor values were spuriously large ("pumped up"; **Karweit, 1974**).

Because significant wave-induced stresses can interact nonlinearly with the quasi-steady stresses (Smith, 1977; Grant and Madsen, 1979) and thus modify equation (1b), it is important to identify periods of significant wave activity during the experiment. Variance estimates of the current speed were

computed to indicate these periods **of increased wave activity**.

Shear velocity u^* and bottom roughness Z . were determined **for each** hourly **set** of one-minute averages **of** current speeds s by fitting to a least-squares curve, using equation (1b) to the e-m the current-meter data obtained at the four heights. A regression coefficient r and standard error were also computed for each least-squares curve.

RESULTS

During fair-weather periods, bottom currents at the **GEOPROBE** site (Fig. 1) were characterized by mixed rotary tidal currents strongly polarized in a **WNW-ESE** orientation and by a weaker northerly mean flow. During stormy periods, moderate northerly wind-driven bottom currents and intense oscillatory wave currents were also observed (**Cacchione** and Drake, 1980). Figure 2 shows part of the current record taken with the e-m current meter at 100 cm above the sea floor. The mixed-tidal oscillations and **fortnightly tidal cycle are readily apparent in the speed data**. **The east-west** current speeds are larger than the north-south current speeds and contain a pronounced diurnal periodicity. Harmonic tidal analysis shows that the K_1 tidal constituent is the most energetic and that the K_1 tidal ellipse has pronounced **WNW-ESE** orientation; the ratio of major to **minor** axis length of this ellipse (**K_1**) is about **10:1**. The relatively low daily averages ("sticks") in curve **cm 1** (Fig. 3) indicate a generally weak northerly flow (about **3** cm/s). Tidal and higher frequency motions **in** the current data have been removed from the daily mean currents (Q). The **nontidal** northerly current on **July** 25 and 26 was associated with an increase **in** wind speed. The effects of this event on the

computations of u_* are discussed later.

The variance of current speeds for each e-m current meter over the period July 8-September 8 are plotted in Figure 3. Significant increases in variance estimates above generally low values occur infrequently, **most** notably on July **25 and after September 1** (Fig. 3). The higher variance values on July 25 correspond to the higher nontidal daily-averaged currents shown in Figure 2. Late on July 24, weather records from the National Weather Service, **None, indicate that** hourly wind speeds increased to 15 to 20 knots; these higher winds persisted until early on July 26. Wind directions were persistently from the south-southeast throughout that time. The bottom pressure data taken on the **GEOPROBE** during this period indicate that wind waves increased on July 25 to about 1-m heights (data not shown), with corresponding wave-induced peak current speeds of about 15 cm/s (measured with the e-m current meter at 1 m above the sea floor). These wave currents were the highest recorded during the period July 8-September 1. After September 1, the energy levels in **wave-**induced bottom currents increased substantially in response to the more frequent **passage** of intense storms. The high variance values during the period September 3-8 were caused by high wave currents (Fig. 3).

Hourly values of u^* and current speed at 100 cm above the sea floor (u_{100}) are shown in Figure 4. Higher values of u_* and U_{100} regularly occur during spring tides at peak values of about 3.5 and 33 cm/s, respectively. The fortnightly rhythmic pattern in these parameters is also easily discernible in Figure 4. The bottom roughness Z_0 has a more irregular variation not readily correlated with the spring-neap cycle. The reason for this erratic variation in measured Z_0 is unknown; however, as discussed

earlier, sediment transport during periods when $u_* > u_{*c}$ could significantly alter the value of z_0 (Smith, 1977). The estimated value of U_* for surface deposits at the GEOPROBE site is about 1.3 cm/s (mean grain size is 70 μm); (Cacchione and Drake, 1979). This value of u_{*c} was derived from the modified Shield's curve shown by Smith (1977), applicable for uniform flow over a noncohesive sediment bed. The drag coefficient C_D , computed from $\frac{(u_*)^2}{U_{100}^2}$, is plotted for comparison with previous estimates (for example, Sternberg, 1968; McCave, 1973).

DISCUSSION

Although the computation of u^* and Z was carried out for each of the hourly sets of e-m data points, as discussed above, it is useful to examine the accuracy of fitting a curve (in the least-squares sense) using equation (1b) to the burst-averaged speed data. A summary of correlation coefficients r , which are estimates of the goodness of fit of the least-squares curve to the data points (Davis, 1973), is shown in Table 1. The large number (approx. 80 percent of r values greater than 0.8) indicates the generally good fit of the least-squares curve given by equation (1b) to the entire data set. This result implies that hourly velocity profiles in this shelf region are dominantly logarithmic.

Figure 5 plots the relation of r^2 and U_{100} . In general (except for about 5 data points in the middle of the diagram), low values of r^2 occur at the low values of u_{100} (<10 cm/s); conversely, high values of r^2 predominantly are correlated with high values of U_{100} (≥ 10 cm/s). This result suggests that the vast majority of poor logarithmic fits to the data occur at times of low

currents. **This** result is not surprising because **low bottom** currents, like periods of light surface winds, could be expected **to** vary considerably in both speed and direction in the bottom boundary **layer** and thus **to** deform the velocity profile.

We have already shown that the measured u^* values at times exceed U_c^* (1.3 cm/s)* Figure 4 indicates **that significant bottom-sediment movement at the GEOPROBE site occurs on a fortnightly cycle, during periods of spring tides.** Evidence for this rhythmic pattern of sediment movement associated with the tidal cycles during fair weather is **also** found in the bottom photographs and light-scattering measurements taken with the GEOPROBE. In particular, the turbidity in the water at about 2 m above the sea floor (as detected with the GEOPROBE **nephelometer**) increases and decreases with the spring and neap cycles, respectively. During peak spring tides, bottom photographs are totally obscured by the increased turbidity of the water. Since the critical bottom stress is exceeded during spring tides (Fig. 4), local resuspension of bottom material probably occurs, and the increased turbulence causes upward mixing of the suspended materials. This mixing could create a bottom turbid layer that diminishes and thins during times of low u^* (**neap** tides). Turbid bottom layers (**nepheloid** layers) have been reported in other continental-shelf areas (Drake, 1976; Pak and **Zaneveld**, 1977), although their precise mechanism is unresolved.

We **note both the** varying and periodically high values of measured Z . (**Fig. 4**). The average **value of z_0** for the period July 8-September 8 was about 2.2 cm; similar high values of Z . have been reported for tidally dominant flows using current-meter-profile data (**Kagan**, 1971). Measurements of Z . in a

shallow-marine environment also show considerable scatter (from 10^{-6} to 10^1 cm) in any one locality over a range of hydraulic-flow conditions (Heathershaw, 1976).

The actual physical bottom roughness at the **GEOPROBE** site was difficult to determine from bottom photographs because of the high turbidity. Shipboard underwater television and **70-mm** bottom photographs taken two days after deployment of the **GEOPROBE** reveal a sedimentary surface characterized by low animal-generated mounds and burrows, with typical horizontal scales of 2 to 20 cm and vertical scales of 1 to 10 cm. The largest number of these features appear to protrude about 4 to 8 cm above the general bed level. A few isolated short-crested incipient sediment ripples also are scattered about the **GEOPROBE** site. The infrequent occurrence of ripples in this area is probably due to the relatively high silt content of the surface deposits and the active destruction of these features by the abundant organisms. If a physical roughness k_s of 6 cm is used to represent the bed, Z_o , estimated from $v_o = k_s/30$ (hydraulically rough flow), would be about 0.2 cm (Schlichting, 1968), a value ten times smaller than the mean measured value of Z . determined from the velocity profiles. The reason for this discrepancy is unknown, but the estimate for k_s here is based on an extremely limited number of photographic observations of low accuracy. Other researchers have reported large values of measured Z . based on velocity-profile measurements on continental shelves (Scott and Csanady, 1976).

As pointed out earlier, Smith and McLean (1977) showed that Z . should be proportional to the excess shear stress when bed-load transport is occurring:

$$z_o = \frac{\alpha_o(\tau_b - \tau_c)}{(\rho_s - \rho)g} + z_N; \tau_b \geq \tau_c, \quad (4)$$

where $\tau_c = \rho u_{*c}^2$, ρ_s is the density of the local sediment, g is the gravitational acceleration, z_N is the Nikuradse roughness (Schlichting, 1968), and α_o is an empirically determined constant (Smith and McLean, 1977). α_o was estimated to be 26.3 by Smith and McLean (1977) on the basis of their velocity-profile measurements in the Columbia River.

Equation (4) can be rewritten:

$$z_o = 1.63 \times 10^{-2}(u_{*b}^2 - 1.69) + z_N, \quad (5)$$

when $\rho_s = 2.65 \text{ g/cm}^3$, $\alpha_o = 26.3$, and $u_b = 1.3 \text{ cm/s}$. Apparently the values of Z computed from equation (5) are considerably below the peak values shown in Figure 4. For example, using a value of $u_{*b} = 3.5 \text{ cm/s}$, $(z_o - z_N)$ as determined from equation (5) is about 0.2. If z_N is about 0.2 cm (see above), Z is about 0.4 cm.

Large variations in c_D have also been reported previously (Heathershaw, 1976). Sternberg (1968), using velocity data obtained in six tidal channels in Puget Sound, Washington, over a wide range of flow and bottom conditions, calculated a mean c_D value of 3.1×10^{-3} ; the range in c_D values was from 0.57×10^{-3} to 11.1×10^{-3} . The mean value of c_D , using the data shown in figure 4, is 10×10^{-3} . We note that high values of c_D (and Z_o) are correlated with low values of U_{100} (Fig. 4).

Finally, the relatively large values of u_* and U_{100} on July 25 are a result of the increased current speeds and bottom stresses caused by wind-

driven currents and surface waves. Measured oscillatory currents during the period July 25-26 had peak speeds of 15 cm/s at 100 cm above the sea floor; the average wave period determined from the burst pressure over 10 consecutive bursts was about 6.8 s. The hourly u_* values (reported in Fig. 4) during the period of increased wave stresses on July 25 (as well as after September) are probably underestimated. Smith (1977) and Grant and Madsen (1979) have shown that oscillatory wave stresses can interact nonlinearly with the quasi-steady stress components to increase the quasi-steady part. This wave-current interaction during the periods of increased wave activity, particularly September 7 to 17, 1977, in Norton Sound, is discussed elsewhere (Cacchione and Drake, 1960).

CONCLUSIONS

More than 80 percent of the measured velocity profiles taken with the GEOPROBE in Norton Sound vary logarithmically with distance above the bottom. Nonlogarithmic profiles generally occur during periods of low currents associated with turning of the tide. Logarithmicity of the profile persisted throughout periods of increased nontidal bottom currents, probably caused by higher local wind stress.

Diurnal and fortnightly variations in u_* and U_{100} appear throughout the measurements. Both c_D and Z also show diurnal periodicities, although no fortnightly cycles are discernible. The values of c_D are higher than previous estimates for tidally dominant flows (Sternberg, 1968; McCave, 1973); however, unlike those of previous studies that were carried out in tidal channels, our measurements were obtained in the mouth of a wide embayment on an expansive

continental shelf. The mean values of C_D and z_0 over the 65-day period were 10×10^{-3} and 2.2 cm, respectively. This mean value of Z is considerably larger than that predicted for hydraulically rough flow over a bottom with irregular random roughness elements of 4- to 8- cm heights.

A distinct bottom nepheloid layer persisted throughout the experimental period; the turbidity and thickness of this layer increased in response to higher values of u_* during peak tidal flows. During maximum tidal currents, and particularly during spring tides, values of u_* exceeding u_{*c} indicate resuspension and transport of bottom materials. The increased turbulence associated with higher u_* values probably caused the near-bottom layer to thicken and to intensify in turbidity. Weaker mean regional flow probably advects the suspended materials northward away from the Yukon prodelta. Apparently, during fair weather this flow removes large amounts of the fine sediment supplied to the region by the Yukon River. Drake and others (1980) discuss the role of regional flow and storm-generated currents in transporting Yukon-derived materials into the Arctic basin.

The data reported here yield the longest continuous estimates of u_* , Z_0 , and C_D yet reported for a bottom boundary layer on an open continental shelf. Similar measurements in other continental-shelf areas, as well as other geologic and geophysical data collected with the GEOPROBE system, should increase our understanding of the response of surface deposits in particular regions to bottom stresses driven by different physical mechanisms.

ACKNOWLEDGMENTS

This work was carried out as part of the marine environmental studies program of the U.S. Geological Survey, Menlo Park, California, and was supported by the Bureau of Land Management through interagency agreement with the National Oceanic and Atmospheric Administration, under which a multiyear program responding to the needs of petroleum development of the Alaskan Continental Shelf is managed by the Outer Continental Shelf Environmental Assessment Program (OCSEAP) office. We thank James Nicholson, George Tate, and Charles Totman for their assistance with the GEOPROBE tripod operation, and Paul Freitag for his technical aid.

REFERENCES

- Bowden, **K. F., Fairbairn, L. A., and Hughes, P.** (1959) The distribution of shearing stresses in a tidal current. **Geophys. Jour. Royal Astronom. Soc., 2**, 288-305.
- Cacchione, D.A. and Drake, D.E. (1979)** A new instrument system to investigate sediment dynamics on continental shelves; **Mar. Geol., 30**, 299-312,
- Cacchione, D.A. and Drake, D.E. (1980)** Storm-generated sediment transport on a shallow continental shelf. **J. Geophys. Res.,** in press.
- Davis, J.C. (1973)** Statistics and Data Analysis in Geology. John Wiley & Sons, New York, 550 pp.
- Drake, D.E. (1976)** Suspended sediment transport and mud deposition on continental shelves. In: Marine Sediment Transport and Environmental Management. (Ed. by **D.J. Stanley and D.J.P. Swift**), John Wiley and Sons, New York, 127-158.
- Drake, D.E., Cacchione, D.A., Muench, R.D., and Nelson, C.H. (1980)** Sediment transport in Norton Sound Alaska. **Mar. Geol.,** in press.
- Grant, W.D. and Madsen, O.S. (1979)** Combined wave and current interaction with a rough bottom. **J. Geophys. Res., 84 (C4)**, 1797-1808.

- Heathershaw, A.D.** (1976) Measurements of turbulence in the Irish Sea benthic boundary layer. In: The Benthic Boundary Layer (Ed. by I.N. McCave), Plenum Press, New York, 11-31.
- Kagan, B.A.** (1971) Sea bed friction in a one-dimensional tidal current. *Izvestiya, Atmos. and Oceanic Phys.*, **8**, 780-785.
- Karweit, M.** (1974) Response of a Savonius roter to unsteady flow. *J. Mar. Res.*, **32**, 359-364.
- McCave, I.N.** (1973) some boundary-layer characteristics of tidal currents bearing sand in suspension. *Memoires Societe Royale des Sciences de Liege*, 6th series, VI, 187-206,
- Pak, H. and Zameveld, J.R.V.** (1977) Bottom nepheloid layers and bottom mixed layers observed on the continental shelf off Oregon. *J. Geophys. Res.*, **82** (27), 3921-3931.
- Schlichting, H.** (1968) Boundary-Layer Theory. McGraw Hill, New York, 748 pp.
- Scott, J.T. and Csanady, G.T.** (1976) Nearshore currents off Long Island, J. *Geophys. Res.*, **81** (30), 405-409.
- Smith, J.D.** (1977) Modeling of sediment transport on continental shelves. In: *The sea: Marine Modeling* (Ed. by Goldberg, E.D., McCave, I.N., O'Brien, J.J., and Steele, J.H.), Wiley-Interscience, New York, 539-577.

smith, J. D., and McLean, **S.R.**(1977) Spatially averaged flow over a wavy surface. **J. Geophys. Res.**, **82 (12)**, 1735-1746.

Sternberg, RoW. (1968) Friction factors in tidal channels with differing bed roughness. **Mar. Geol.**, **6**, 243-260.

Wimbush, M. (1976) The physics of the benthic boundary layer. In: The Benthic Boundary Layer (Ed by **I.N. McCave**), Plenum Press, New York, 3-10.

Table 1. Distribution of correlation coefficients (r) determined from a linear least-squares fit to the GE RO hourly current profiles, Sound, Alaska.

	1.00	0.90	0.80	0.70	0.60	0.50	0.40	0.30	0.20	0.10	0.0	<0*
Number of occurrences-----	1210	362	113	60	33	28	19	16	10	9	60	
Percentage of occurrences-----	63	19	6	3	2	1	1	<1	<1	<1	3	

* Values of r < 0 indicate profiles whose slope was negative; i.e., velocity as taken from the fitted least-squares straight line decreased from the lowest level z = 20 .

Figure Captions

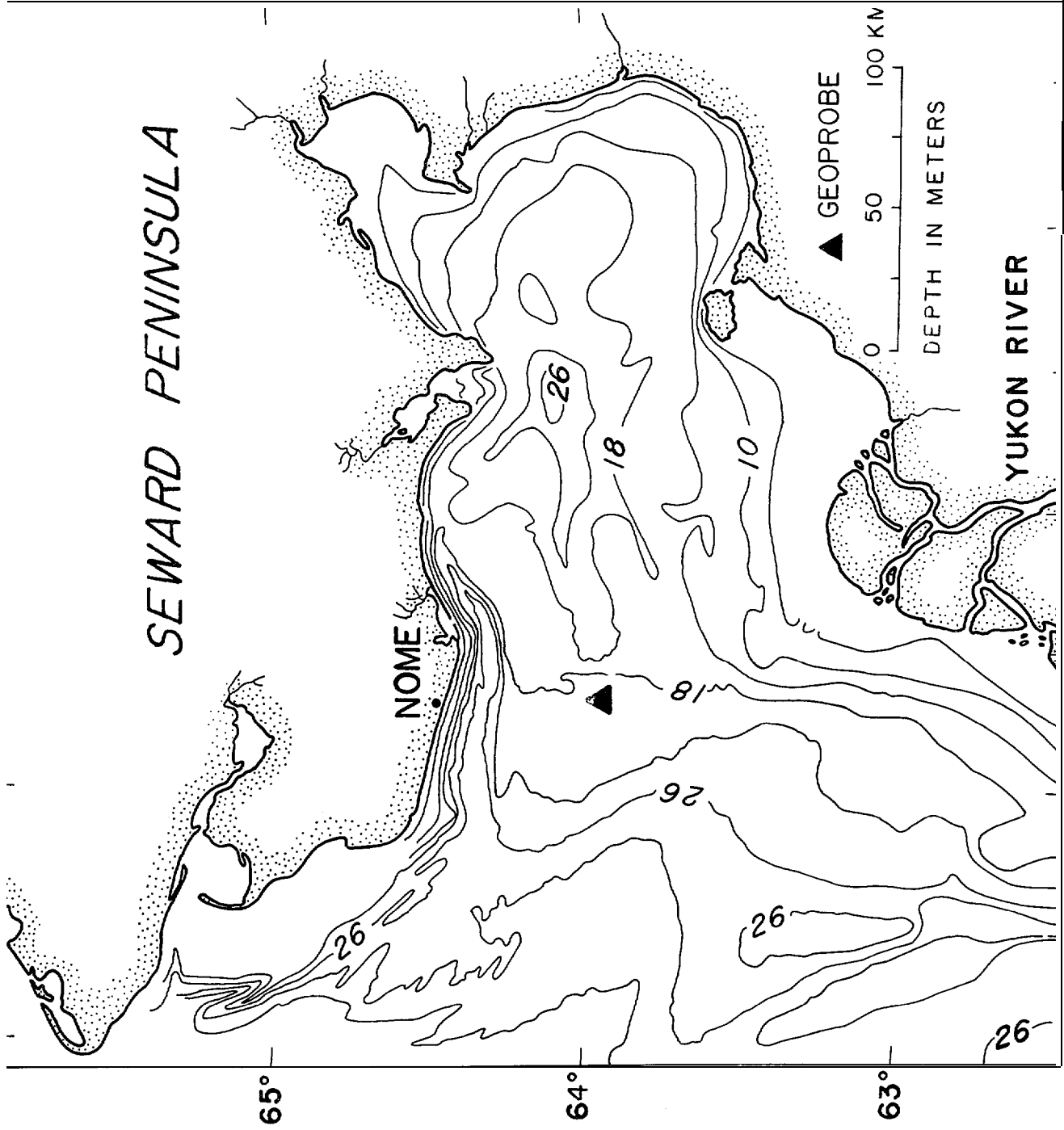
Fig. 1. Bathymetric **chart** of Norton Sound, Alaska, showing location of **GEOPROBE** (A) during July-September 1977.

Fig. 2. Time series of currents measured at 100 cm above sea floor with GEOPROBE e-m current meter, showing variations in current speed U_{100} (a); current direction (b), east(+)-west(-) component u (c), , north(+)-south(-) component v (d), and daily-averaged speed vectors ("sticks").

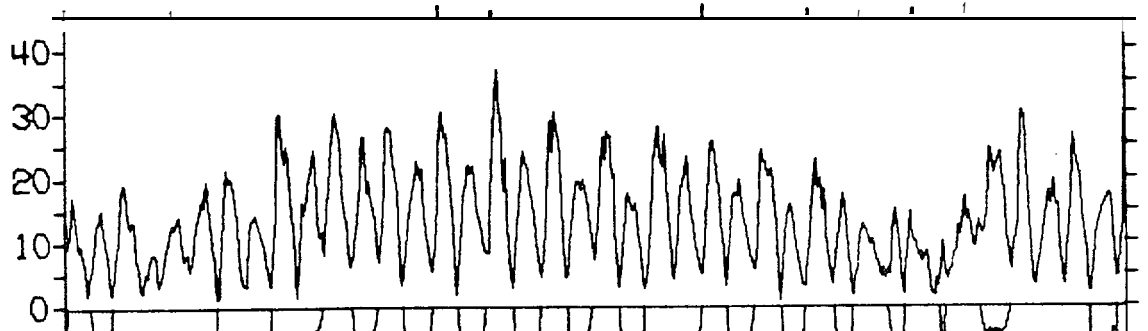
Fig. 3. Variance of burst-averaged current speeds for GEOPROBE e-m current meters at 20 (cm1), 50 (cm2), 70 (cm3) and 100 (cm4) cm above sea floor. Horizontal axis is marked at 4-day intervals.

Fig. 4. Time-series values of shear velocity (u_*), current speed at 100 cm above sea floor (u_{100}), drag coefficient (CD), and roughness (z_0) during period July 8-September 10, 1977. Horizontal axis is marked at 6-day intervals.

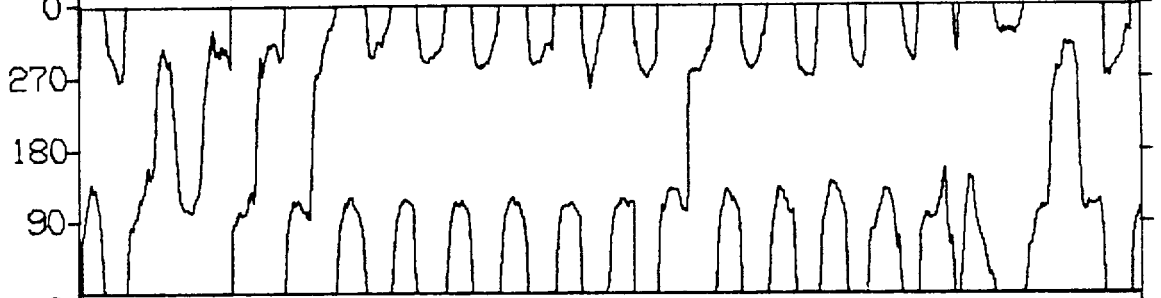
Fig.5. Square of correlation coefficient (r^2) obtained for least-squares-fitted curves to current-meter data and current speed at 100 cm above bottom (u_{100}).



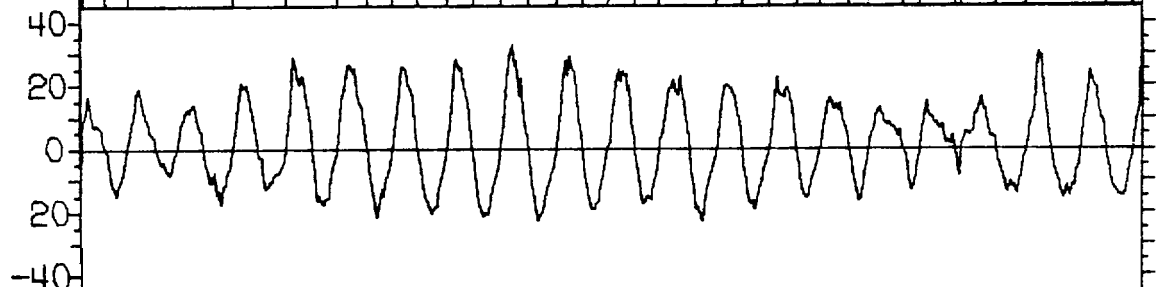
U_{100}
cm/s)



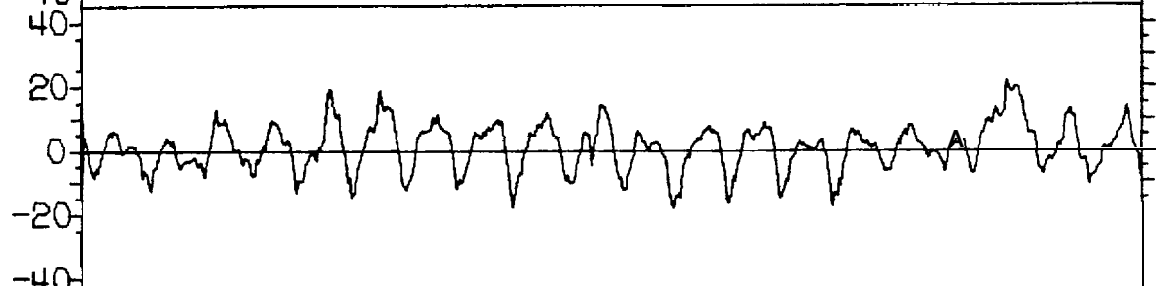
Θ
deg)



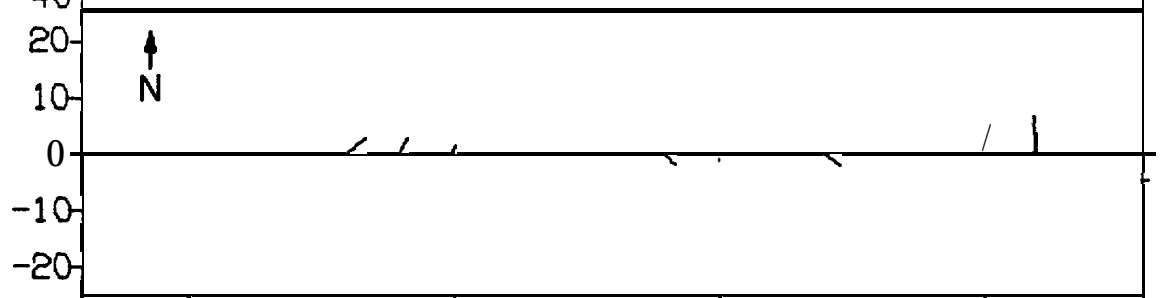
\bar{u}
cm/s)



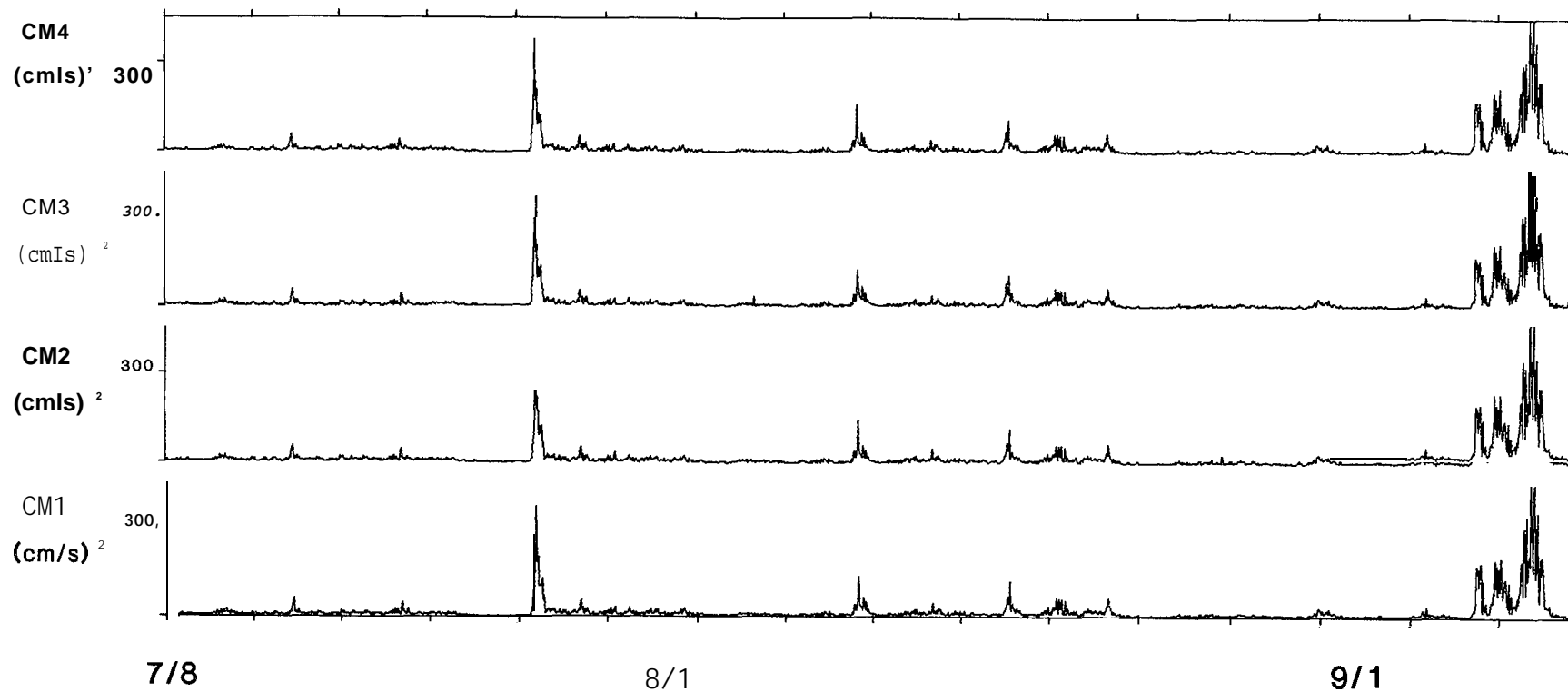
V
cm/s)



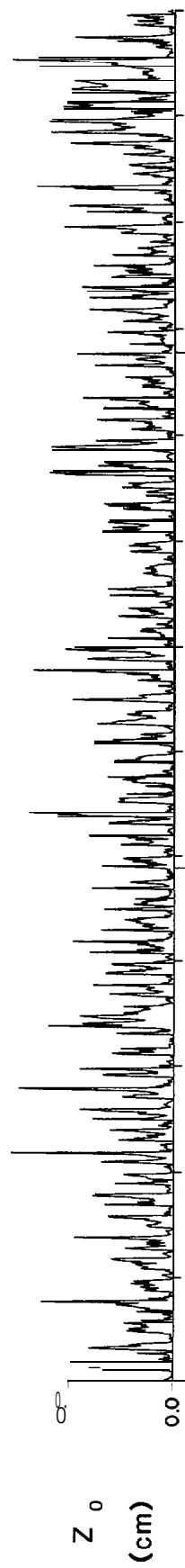
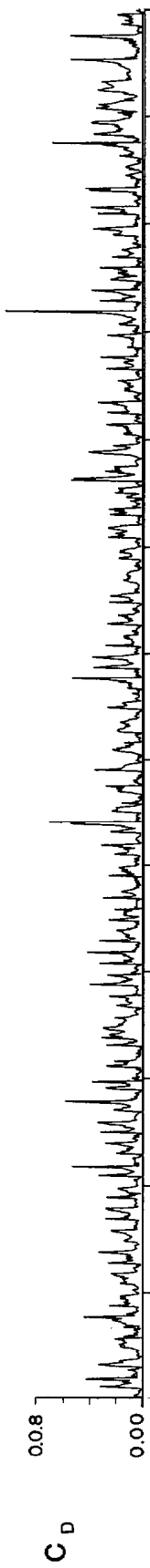
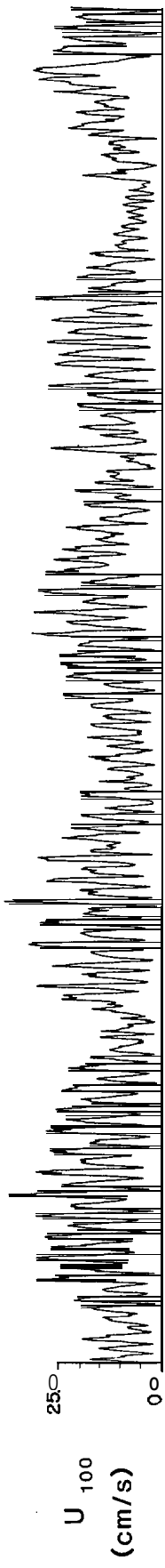
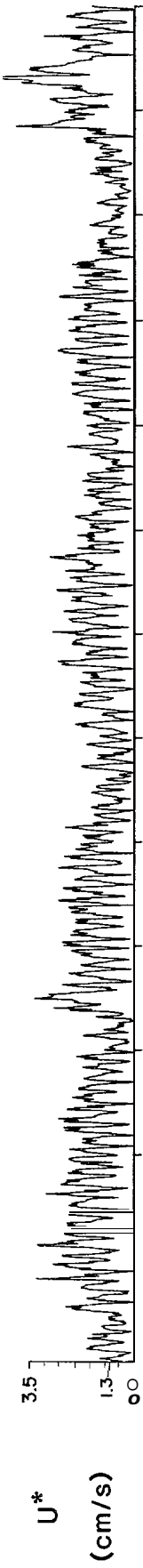
Q
cm/s)



8 10 15 20 25
JUL-77



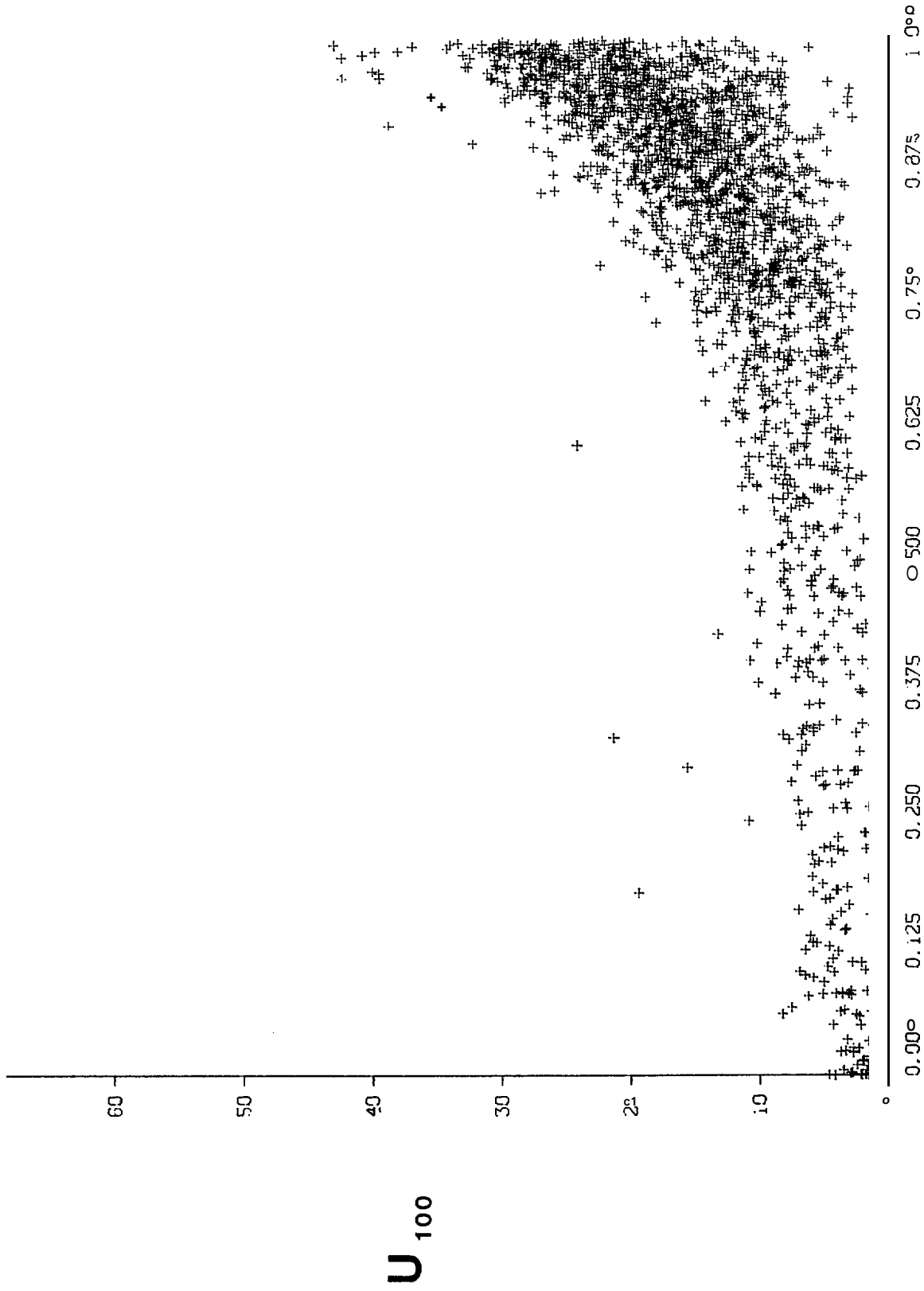
NOPTON SOUND 1977



JULY 8

AUG 1

SEPT 1



REGRESSION COEFFICIENT - R SQUARED